Research Article / Araştırma Makalesi
doi: 10.18678/dtfd.1653329

Duzce Med J, 2025;27(3):279-291
Düzce Tıp Fak Derg, 2025;27(3):279-291

Impact of Promoter-Independent CpG-Rich A2UCOE Subregions on Transgene Expression

Promotör Bağımsız CpG Zengini A2UCOE Alt Bölgelerinin Transgen Ekspresyonu Üzerine Etkisi

Ali Osman ARSLAN
0000-0002-5711-0038
Ömer Faruk ANAKÖK
0000-0002-5747-9644

Department of Medical Biology, Abant İzzet Baysal University Faculty of Medicine, Bolu, Türkiye

Corresponding Author
Sorumlu Yazar
Ali Osman ARSLAN
aliosmanarslanist@hotmail.com

Received / Geliş Tarihi : 07.03.2025
Accepted / Kabul Tarihi : 12.09.2025
Available Online / Çevrimiçi Yayın Tarihi : 07.10.2025

ABSTRACT

Aim: This study aimed to evaluate the ability of CpG-rich subregions within the A2UCOE element, excluding the HNRPA2B1 and CBX3 promoters, to sustain long-term transgene expression in lentiviral systems. These regions are cloned upstream of the spleen focus-forming virus (SFFV) promoter and tested in P19 and F9 cells.
Material and Methods: The study assessed the ubiquitous chromatin opening element (UCOE) activity of three A2UCOE subregions that lack promoters. Using P19 and F9 murine embryonal carcinoma cells, enhanced green fluorescent protein (eGFP) expression stability and durability were examined in undifferentiated and differentiated states. Lentiviral vectors (LVs) containing CpG-rich, promoterless fragments, 455UCOE (OFA1), 527UCOE (OFA2), and 945UCOE (OFA3), were transduced into the cells, and sustained transcriptional activity was analyzed via flow cytometry.
Results: Some vectors sustained eGFP expression, while others exhibited a rapid decline in both undifferentiated and differentiated states. Specifically, the OFA1, OFA2, and OFA3 vectors showed trends similar to the SEW vector, with significant reductions in eGFP expression over time. None of the CBX3-derived fragments provided stable expression, suggesting no UCOE activity. The rates of expression decline were similar between the SEW vector with the SFFV promoter and the LVs containing OFA1, OFA2, and OFA3.
Conclusion: CpG-rich, promoterless fragments failed to support stable transgene expression in murine embryonal carcinoma cells, indicating a lack of UCOE functionality. These findings highlight the role of promoter and regulatory elements in maintaining open chromatin for gene therapy. Future studies should investigate other CpG-rich regions or minimal promoters to improve transgene stability.
Keywords: Promoter activity; UCOE function; transcriptional silencing; SFFV promoter; gene expression stability.

ÖZ

Amaç: Bu çalışmanın amacı, HNRPA2B1 ve CBX3 promotörleri hariç olmak üzere, A2UCOE elemanındaki CpG zengin alt bölgelerin lentiviral sistemlerde uzun süreli transgen ekspresyonunu sürdürme yeteneğini değerlendirmektir. Bu bölgeler spleen focus-forming virüs (SFFV) promotörünün önüne klonlanmış ve P19 ile F9 hücrelerinde test edilmiştir.
Gereç ve Yöntemler: Bu çalışmada, promotör içermeyen üç A2UCOE alt bölgesinin ubiquitous chromatin opening element (UCOE) aktivitesi değerlendirildi. P19 ve F9 fare embriyonal karsinom hücreleri kullanılarak, farklılaşmamış ve farklılaşmış durumlarda enhanced green fluorescent protein (eGFP) ekspresyon stabilitesi ve dayanıklılığı incelendi. CpG zengin, promotörsüz fragmanlar içeren lentiviral vektörler (LV'ler), 455UCOE (OFA1), 527UCOE (OFA2) ve 945UCOE (OFA3) hücrelere aktarıldı ve akım sitometrisiyle sürekli transkripsiyonel aktivite analiz edildi.
Bulgular: Bazı vektörler eGFP ekspresyonunu sürdürürken bazıları ise hem farklılaşmamış hem de farklılaşmış durumlarda hızlı bir azalma gösterdi. Özellikle OFA1, OFA2 ve OFA3 vektörleri, SEW vektörüne benzer eğilimler göstererek zamanla eGFP ekspresyonunda belirgin azalmalar sergiledi. CBX3 kökenli fragmentlerin hiçbiri stabil ekspresyon sağlamadı, bu da UCOE aktivitesinin olmadığını düşündürdü. Ekspresyon azalma hızları, SFFV promotörlü SEW vektörü ile OFA1, OFA2 ve OFA3 içeren LV'ler arasında benzerdi.
Sonuç: CpG zengin, promotör içermeyen fragmanlar fare embriyonal karsinom hücrelerinde stabil transgen ekspresyonunu destekleyememekte, bu da UCOE fonksiyonelliğinin olmadığını göstermektedir. Bulgular, gen terapisi için açık kromatinin korunmasında promotör ve düzenleyici elemanların önemini vurgulamaktadır. Gelecek çalışmalar, transgen stabilitesini artırmak için alternatif CpG zengin bölgeler veya minimal promotörleri araştırmalıdır.
Anahtar kelimeler: Promotör aktivitesi; UCOE fonksiyonu; transkripsiyonel susturma; SFFV promotörü, gen ekspresyon stabilitesi.

INTRODUCTION

Gene therapy is an innovative approach to treating inherited disorders by delivering therapeutic nucleic acids to target cells. These nucleic acids aim to correct genetic mutations or regulate gene expression, addressing various pathological conditions (1). Delivery methods are classified as viral and non-viral. Viral vectors use viruses' natural ability to transfer genes, while non-viral methods employ liposomes or carriers to deliver DNA into cells (2,3). Advancements in genetic engineering have optimized viral vectors, improving the use of recombinant viral platforms in research and clinical therapies (4,5).

Lentiviral vectors (LVs), derived from HIV-1, are widely used RNA-based delivery systems in gene therapy. They are highly effective at targeting neurological tissues, liver parenchyma, and dormant progenitor cells due to their ability to infect both proliferative and quiescent cells (6). LVs have an adaptable structure and can encapsulate around 8 kilobases of genetic material. Their versatility is further enhanced by pseudotyping, which adds heterologous viral glycoproteins for targeted cell and tissue delivery (7). Recombinant viral vectors carry risks such as viral recombination or unintended genome integration, potentially causing unregulated gene expression or replication-competent virus emergence, especially in natural HIV-1 infections. To reduce these risks, self-inactivating (SIN) LVs have been developed to minimize transcriptional interference and mutagenesis (8,9).

Gene silencing is a major challenge in gene therapy. Retroviral vectors often face transcriptional repression and expression variability after integrating into host cell genomes (10,11). This phenomenon is mainly driven by CpG dinucleotide methylation and post-translational histone modifications. These modifications compact chromatin and hinder stable transgene expression (12,13). Despite extensive characterization of ubiquitous chromatin opening elements (UCOEs) and their role in counteracting gene silencing, a key limitation in many studies is the lack of comprehensive epigenetic profiling. This includes analyses such as DNA methylation mapping and histone modification assessment. This study is also limited by the absence of comprehensive epigenetic profiling. These epigenetic data are critical for elucidating the underlying mechanisms that explain why promoterless CpG-rich sequences may fail to sustain chromatin opening and UCOE activity. Without such analyses, interpretations of UCOE functionality remain incomplete.

To address gene silencing challenges, researchers have incorporated UCOEs into expression constructs. UCOEs efficiently mitigate gene repression induced by heterochromatin assembly, enabling sustained and enduring transgene manifestation in mammalian cell platforms (14,15). A2UCOE, derived from the human HNRPA2B1-CBX3 locus, is a chromatin-opening element with an unmethylated CpG island and dual promoters. It enhances gene expression stability by reducing transgene silencing, even in heterochromatic regions (16,17). The A2UCOE mechanism depends on two key elements: i) a non-methylated CpG-rich domain, and ii) the bidirectional transcriptional activity of the HNRPA2B1 and CBX3 promoters. This framework has been rigorously assessed both in vitro and in vivo, including within murine hematopoietic stem cells (HSCs), where it exhibited consistent stability and replicability (18). By effectively neutralizing gene silencing induced by DNA methylation, A2UCOE substantially amplifies transgene expression levels.

Although CpG density is important for UCOEs, recent studies show that CpG richness alone cannot maintain open chromatin or prevent silencing. For example, the absence of active transcriptional processes and recruitment of specific chromatin remodelers may limit the chromatin opening effect of CpG islands (19,20). Histone modifications like H3K27 acetylation and H3K4 methylation, together with chromatin remodeling complex interactions, are essential to keep chromatin accessible (21). Therefore, without promoter activity and associated transcription factor binding, CpG-rich sequences may fail to recruit these epigenetic regulators, leading to eventual gene silencing despite high CpG content (22). This emphasizes the necessity of comprehensive epigenetic profiling, including DNA methylation and histone modification analyses, to fully understand UCOE functionality and to design improved chromatin-opening elements.

The efficacy of the A2UCOE construct is assessed through CpG-rich regions and bidirectional enhancers, leading to the identification of improved UCOE candidates for gene therapy. Incorporating chromatin-modifying elements like A2UCOE into lentiviral systems can enhance gene therapy by reducing silencing and sustaining transgene expression. Elucidating the structure and function of A2UCOE regions may enhance LV design, promoting safer, more effective gene therapies and advancing regenerative and precision medicine (14).

A study conducted by Thomson et al. (23) revealed that a transgene comprising a CpG-enriched DNA segment, devoid of promoter elements, could establish an unmethylated domain even in the absence of RNA polymerase II, while concurrently facilitating active histone modifications. However, further epigenetic analyses, including DNA methylation profiling and chromatin accessibility assays, are essential to clarify why CpG density alone might be insufficient to confer a chromatin opening function. Addressing this gap will provide a more comprehensive understanding of UCOE activity and inform the design of improved chromatin-opening elements.

To achieve this, a genomic region just downstream of the two initial exons of CBX3 was selected, meeting the criteria (Figure 1). The 945 bp segment was then split into two fragments, 455 bp and 527 bp; 455UCOE (OFA1), 527UCOE (OFA2), and 945UCOE (OFA3). Each fragment was independently cloned upstream of the spleen focus-forming virus (SFFV) promoter in the SEW vector, a lentiviral construct containing the SFFV promoter, the enhanced green fluorescent protein (eGFP) reporter gene, and the Woodchuck hepatitis virus posttranscriptional regulatory element (WPRE), as illustrated in Figure 2. The UCOE functionality of these constructs was assessed using mouse-derived embryonic carcinoma cell lines (P19 and F9), which are broadly acknowledged as resilient models for evaluating the prolonged expression of LVs (24,25). Stability, expression levels, and consistency of the eGFP transgene were monitored in both undifferentiated and differentiated P19 and F9 cells.

This study aimed to determine whether CpG-rich, promoterless subregions of the A2UCOE locus could sustain stable transgene expression by resisting epigenetic silencing. This investigation is crucial for improving gene therapy vector design and understanding epigenetic regulation mechanisms.

MATERIAL AND METHODS

In this study, an investigation was conducted to determine whether the three subdivisions of the HNRPA2B1-CBX3 universal chromatin activation element (A2UCOE) retained their functional properties as UCOEs. This work was initiated based on emerging evidence that challenges the requirement for promoter activity in UCOE function. To evaluate UCOE activity within the vectors, murine embryonal carcinoma cell lines P19 and F9, which are well-established models for assessing the stability of transgene expression in viral vectors, were used (24,25). The durability, efficacy, and consistency of eGFP expression in both undifferentiated and differentiated states of P19 and F9 cells were systematically examined.

Quantitative Assessment of Vector Replication Abundance through Genomic Enumeration

To determine whether the reduction in eGFP expression over time resulted from the depletion of vector-positive cells or from lentiviral-induced gene silencing, real-time quantitative PCR (qPCR) was performed on total genomic DNA. This analysis revealed the median number of vector genome copies per cell at multiple time points during the post-transduction culture period. To serve as a calibration standard for vector copy number (VCN) quantification, a monoclonal population with a single integration of the A2UCOE-eGFP LV was generated by limiting dilution of bulk-transduced P19 and F9 cells.

Quantitative PCR (qPCR) Analysis

To determine whether the time-dependent decline in eGFP expression was due to the loss of vector-positive cells or lentiviral silencing, we performed qPCR on genomic DNA to measure average VCN per cell at each post-transduction time point. A single-copy A2UCOE-eGFP LV cell clone, isolated via limiting dilution from bulk-transduced P19 and F9 cells, was used as a reference standard. qPCR was carried out using EvaGreen® qPCR Master Mix (Biotium, CA, USA), in accordance with the manufacturer's instructions. Samples were analyzed in duplicates or triplicates, and the mean values were reported to ensure reproducibility. Target gene expression levels were normalized to the housekeeping gene RPS29 and calculated relative expression using the ΔΔCt method.

Gene-specific primers used in the study were: RPS29 forward primer: 5'-GAGATGCCTCACACGGAGAC-3', reverse primer: 5'-GGGTTGTTTGCCTTTGGGAC-3', BSR forward primer: 5'-GACTCGATCCTCGTCAACGG-3', reverse primer: 5'-ATCTTCGGCCTCTGATCTCCG-3'. Additionally, three independent transfections were performed per vector, with two replicates for each control vector. This experimental design was applied consistently to both P19 and F9 cell lines to ensure reproducibility and comparability.

Determination of Transduction Efficiency via Flow Cytometric Analysis

To assess transduction efficiency, six wells of a 24-well plate were seeded with 1-2 x10^5 HEK293T cells per well and allowed to adhere for 4 hours. Each well was then transduced with serial dilutions of the viral stock, ranging from 1 µL to 1 x10^{-5} µL. Polybrene was added to the medium at a final concentration of 8 µg/mL. One well served as an untransduced negative control.

At least 2 x 10^5 fixed cells per sample were analyzed using flow cytometry to detect GFP fluorescence. Viable cells were

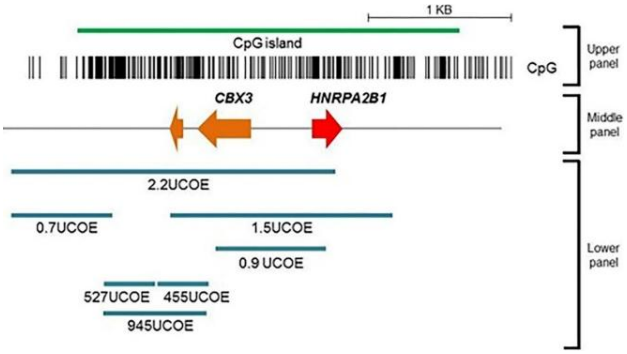


Figure 1. Loci of sub-segments in the A2UCOE domain analyzed for UCOE operability evaluation; **Upper panel:** CpG density distribution with an unmethylated CpG-rich region, **Middle panel:** alternative initiation exons of CBX3 (orange arrows) and HNRPA2B1 gene (red arrow) location, **Lower panel:** functional assessment of A2UCOE segments. 2.2UCOE: regulatory element linked to HNRPA2B1 promoter, 1.5UCOE: positive control interaction with SFFV promoter, 0.7UCOE: the experimental fragment "Daedalus", 0.9UCOE: the MDR region involved in methylation regulation, 945/527/455UCOE: CpG-enriched fragments from the A2UCOE segment tested for gene expression under the SFFV promoter and compared to the 1.5UCOE control, UCOE: ubiquitous chromatin opening element, SFFV: spleen focus-forming virus, MDR: methylation-dependent region

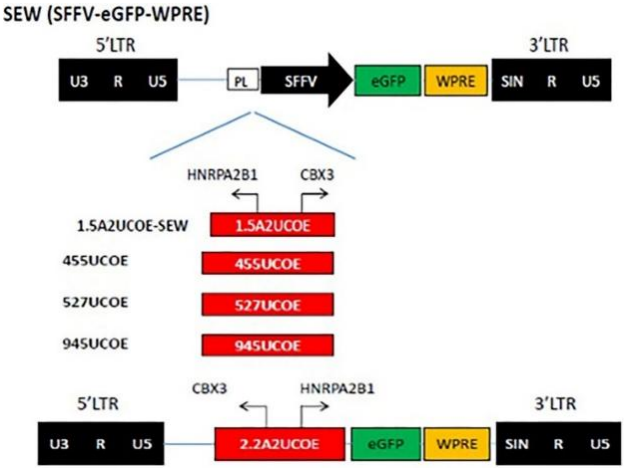


Figure 2. Alternative candidate UCOE and reference LVs; The 1.5 kb HNRPA2B1-CBX3 UCOE (1.5A2UCOE) was integrated into the upstream region of the SFFV promoter at the PL site, creating the 1.5A2UCOE-SEW vector. Similarly, the 2.2 kb HNRPA2B1-CBX3 UCOE (2.2A2UCOE) was ligated with the GFP reporter gene under the control of the HNRPA2B1 promoter, resulting in the 2.2A2UCOE construct. The UCOE sub-fragments analyzed in this study are CpG-rich sequences, with lengths of 455 bp (OFA1), 527 bp (OFA2), and 945 bp (OFA3). These UCOE segments were integrated into the PL region upstream of the SFFV promoter in the SEW vector. UCOE: ubiquitous chromatin opening element, LV: lentiviral vector, PL: polylinker, SFFV: spleen focus-forming virus, eGFP: enhanced green fluorescent protein, WPRE: Woodchuck hepatitis virus posttranscriptional regulatory element, LTR: long terminal repeat

gated based on forward (cell size) and side (granularity) scatter. GFP fluorescence was measured in the FL1 (525 nm) and FL2 (575 nm) channels. Untransduced control samples were used to establish the threshold for GFP positivity, enabling accurate quantification of the percentage of GFP-expressing, viable cells. This value was then used to estimate the multiplicity of infection (MOI) by correlating GFP+ percentages with viral dilution. For reliable MOI estimation, samples with GFP positivity between 1% and 20% were selected. Samples exceeding 20% were excluded to avoid underestimation due to potential multiple viral integrations, while samples below 1% were excluded due to signal noise. Along with the EGFP+ cell numbers in transduced cultures, the actual MOI values were also measured by flow cytometry to correct as given MFI values in graphs. Calculation of the MOI of 1 mL of stock was performed by flow cytometry analysis to determine the percentage of HEK293T cells transduced at each dilution, then scaling the results appropriately to estimate the MOI of the original viral stock.

Preparation of Luria-Bertani (LB) Medium

Luria-Bertani (LB) medium was prepared by dissolving 10 g tryptone, 5 g yeast extract, and 10 g sodium chloride in 1 liter of deionized water. The solution was sterilized by autoclaving at 15 psi for 20 minutes, then cooled to 50°C. Ampicillin was added to a final concentration of 50 µg/mL after cooling, and the medium was stored at 4°C. For LB agar plates, 20 g agar was added per liter of LB medium before sterilization. Selective media were prepared by supplementing the LB medium or agar plates with 100 µg/mL of the appropriate antibiotic.

Effective Conversion of Competent *E. coli* DH5α Strains

Competent *E. coli* DH5α cells, obtained from Life Technologies Ltd., were transformed according to the manufacturer's protocol. Colonies carrying plasmids were cultured overnight at 37°C in a nutrient-rich medium supplemented with 100 µg/mL ampicillin. The transformed colonies were expanded in either small-scale (5 mL) or large-scale (200-500 mL) LB broth containing 100 µg/mL ampicillin. Plasmid DNA was extracted using Qiagen kits, and elution was performed with TE buffer.

Cell Culture Methodology

The HEK293T cell line was maintained in Dulbecco's modified Eagle medium (DMEM) supplemented with 10% fetal bovine serum (FBS), 1%200 mM L-glutamine, and 10 µg/mL penicillin/streptomycin at 37°C and 5% CO_2. 2 x10^7 cells were seeded into T162 culture flasks and transfected when they reached 80-90% confluence. Forty-eight hours after transfection, the culture medium was replaced with fresh DMEM, and it was changed again at 72 hours. For viral titration assays, Cells were plated at a density of 1-2 x10^5 cells per well in 24-well plates and inoculated with serial dilutions of virus, ranging from an MOI of 1 to 1 x10^{-5}. The cells were washed with phosphate-buffered saline (PBS) and dissociated using TrypLE™ solution. The dissociation was neutralized by adding serum-containing medium. For flow cytometric analysis, the cells were fixed in 4% formaldehyde in PBS, homogenized, and they were stored at 4°C in the dark.

For each experiment, three independent transfections were performed per vector, including two different vectors for the control group. The same procedure was applied consistently for both P19 and F9 cell lines.

Culture Conditions for Murine Embryonal Carcinoma Cells

P19 cells were cultured in DMEM supplemented with 2 mM L-glutamine, 1% non-essential amino acids, 10% FBS, and 10 µg/mL penicillin/streptomycin, maintaining them at 37°C in a humidified atmosphere with 5% CO_2. The cells were cultured at 37°C in a moist atmosphere with 5% CO_2. To promote neuronal differentiation, the cells were plated in non-adherent culture plates to support the development of embryoid structures. Subsequently, the cells were exposed to 1 µM all-trans retinoic acid (RA) in DMEM containing 5% FBS. After 2 days of RA treatment, embryoid bodies were dissociated with 0.25% trypsin and 0.53 mM EDTA, re-plated on poly-D-lysine-coated dishes, and differentiated for 2-8 days with 10 µM cytosine arabinoside to enrich non-dividing neuronal cells.

F9 cells were cultivated in gelatin-precoated flasks using DMEM supplemented with 10% FBS, 100 U/mL penicillin, 100 µg/mL streptomycin, and 2 mM L-glutamine. Parietal endoderm differentiation was initiated by treating the cells with 50 nM RA in DMEM/F12 medium supplemented with 5% FBS, thereby promoting the formation of embryoid bodies. After 5-6 days of RA treatment, embryoid bodies were dissociated with 0.25% trypsin and 0.53 mM EDTA, re-plated on poly-D-lysine-coated dishes, and cultured for 2-6 days with 10 µM cytosine arabinoside to enrich non-dividing endodermal cells.

Cell Differentiation and Immunofluorescence Analysis

After differentiation into embryoid bodies, P19 and F9 cells were seeded onto laminin-coated coverslips. Cells were washed with PBS, fixed twice with 4% paraformaldehyde, then permeabilized and blocked with 0.1% Triton X-100 for 30 minutes. Primary antibodies against β-tubulin III (1:200) for P19 and Oct3/4 (1:500) for F9 cells were applied for 1 hour at room temperature in the dark. Following washes, AlexaFluor 488 secondary antibody was incubated for 1 hour. Nuclei were stained with DAPI and Hoechst, coverslips mounted, and samples stored at 4°C. Differentiation was quantified by confocal microscopy detecting β-tubulin III (red) in P19 and Oct3/4 in F9 cells, with DAPI-stained nuclei.

Reporter Gene Analysis

Researchers transduced LV constructs harboring UCOE and A2UCOE eGFP reporter genes into P19 and F9 cell lines. They systematically assessed the expression of the reporter genes during the differentiation process into neural ectodermal and endodermal lineages.

Lentiviral Vectors (LVs) Employed in the Investigation

DNA fragments of 455 bp (OFA1), 527 bp (OFA2), and 945 bp (OFA3), positioned within the initial intron of the CBX3 gene and encompassing CpG-enriched domains, were integrated into the anterior segment of the SFFV promoter within the SEW construct while preserving their native alignment. These fragments were generously provided by our collaborators at University College London, UK. This research extends prior findings indicating that CpG-enriched, promoterless regions are capable of maintaining an accessible chromatin configuration (23). We explored whether the CpG-rich, non-promoter segments of the CBX3 locus, when integrated with the SFFV promoter, could facilitate sustained transcriptional activity. The

spatial arrangement of the A2UCOE subregions under examination was illustrated in Figures 1 and 2.

Selection of Negative and Positive Controls

To assess the impact of UCOE sequences on transgene expression stability, both negative and positive control vectors were included in the experimental setup. The SEW vector, lacking any UCOE element, served as the negative control and is known to rapidly lose transgene expression due to epigenetic silencing following transduction. As a positive control, the 1.5A2UCOE-SEW vector, which incorporates a 1.5 kb A2UCOE fragment previously shown to provide resistance to silencing, was utilized. Additionally, a second positive control vector containing a 2.2 kb A2UCOE fragment was used, as it also confers robust protection against epigenetic repression. The use of these controls allowed a comparative evaluation of the silencing resistance offered by different UCOE fragment lengths under identical experimental conditions. The structures of alternative candidate UCOEs and reference LVs, along with the loci of sub-segments within the A2UCOE region, were depicted in Figures 1 and 2.

The foundational architecture of the conventional SIN LV incorporates the SFFV promoter, which facilitates the transcription of the eGFP as a marker gene. This arrangement is additionally enhanced by the incorporation of the WPRE, which acts as a mediator of post-transcriptional processes. The UCOE vectors examined in this investigation are derived from this foundational design.

Statistical Analysis

All statistical analyses were performed using JASP 0.19.1, and plots were drawn by Python 3.11.5. Code snippets were run on Jupyter Notebook 6.5.7. The primary quantitative outcomes included the proportion of GFP+ cells, mean fluorescence intensity (MFI), and VCN per cell, obtained via flow cytometry and qPCR, respectively. Prior to group comparisons, the distribution of the data was assessed for normality using the Shapiro-Wilk test. Homogeneity of variances was evaluated using Levene's test. For comparisons of independent groups, ANOVA was used if assumptions were satisfied. When the homogeneity assumption wasn't provided, Welch's transformation was performed. In cases where normality was violated, the Kruskal-Wallis test was applied. When significant differences were detected, post-hoc multiple comparison analyses were conducted to determine which groups caused these differences. The Bonferroni test was applied for parameters meeting normality assumptions, while the Dunn test with Bonferroni correction was used for parameters distributed non-normally. A two-tailed p-value of less than 0.05 was considered statistically significant.

RESULTS

The effects of promoter-independent, CpG-rich A2UCOE subregions (1.5A2UCOE and 2.2A2UCOE) were evaluated comparatively alongside newly designed LVs, 455UCOE, 527UCOE, and 945UCOE under both differentiated and undifferentiated conditions in F9 and P19 cell lines. Cells were transduced at MOI of 3 and 6, respectively, and transgene expression was assessed by the percentage of eGFP+ cells, and MFI, as well as VCN, were quantified via flow cytometry and qPCR from day 3 to day 31 (Figure 3). These parameters provided critical insights into the stability of transgene expression and the persistence of vector integration. The MFI, eGFP+ cell percentages, and VCN measurements for differentiated and undifferentiated F9 and P19 cells were presented in Tables 1 to 4.

F9 Cell Line Findings

Undifferentiated F9 Cells

The SEW control vector (lacking UCOE) exhibited high initial expression levels in undifferentiated F9 cells by day 3. However, by day 31, both MFI and eGFP+ percentages

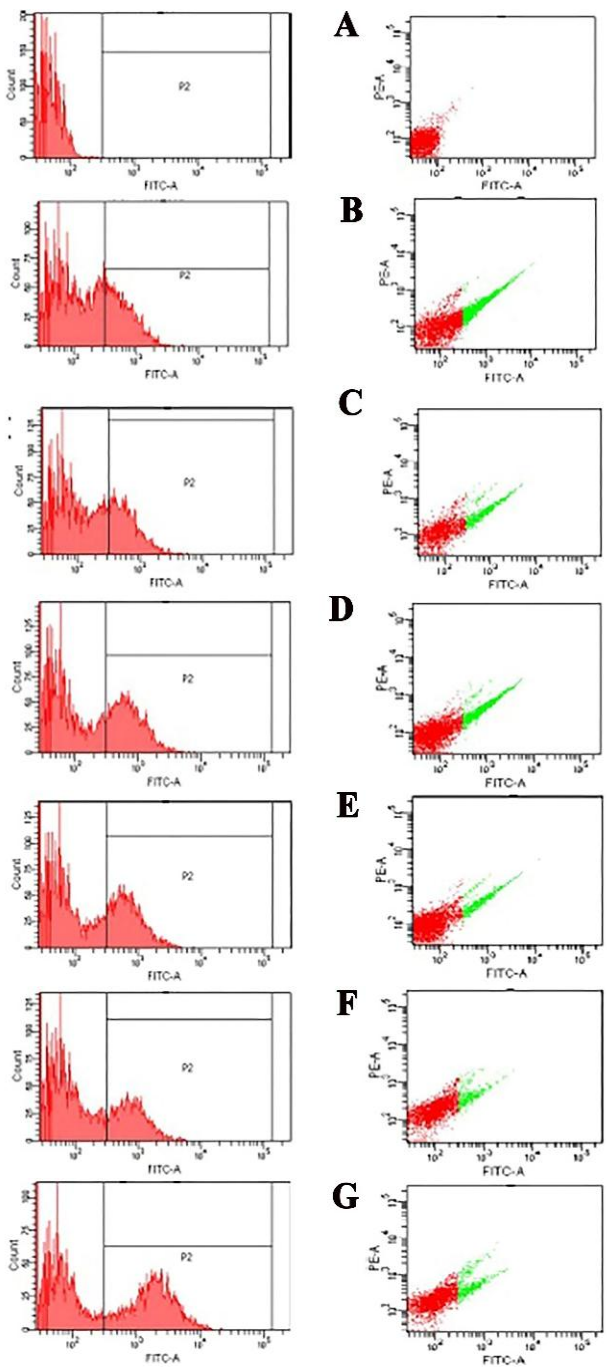


Figure 3. Flow cytometry of non-transduced and transduced P19 and F9 cells before differentiation; **A)** untreated cells from the negative control group, **B)** cells transduced with the SEW vector, **C)** cells transduced with the 1.5A2UCOE-SEW vector, **D)** cells transduced with the 2.2A2UCOE vector, **E)** cells transduced with the OFA1 vector, **F)** cells transduced with the OFA2 vector, and **G)** cells transduced with the OFA3 vector. Flow cytometry was conducted 72 hours after transduction, GFP-negative cells were marked in red, whereas GFP+ cells were distinguished in green

had declined to undetectable levels. Despite this, the presence of the transgene was still detectable in VCN measurements (1.98±0.20, p<0.001). The slight decrease in VCN over time is considered an expected outcome during prolonged culture of transduced cells (Table 1). These findings indicate that transgene loss and transcriptional silencing are more pronounced in vectors lacking UCOE sequences, suggesting that the absence of UCOE results in a lack of protection against epigenetic repression.

eGFP expression in SEW-transduced cells declined by approximately 80% within two weeks post-transduction, whereas OFA1, OFA2, and OFA3 constructs showed a comparatively moderate decrease of 60-70%; this trend was further supported by MFI measurements, which remained stable for 1.5A2UCOE-SEW and 2.2A2UCOE constructs but fluctuated significantly in SEW, OFA1, OFA2, and OFA3 groups, and was additionally substantiated by qPCR-based quantification of VCN per cell using genomic DNA isolated at each time point (Figure 4).

LVs carrying the 1.5A2UCOE and 2.2A2UCOE control elements demonstrated a marked superiority in maintaining transgene expression, as expected. Notably, in cells transduced with the 2.2A2UCOE vector, the MFI, percentage of eGFP+ cells, and VCN at day 31 were measured as 81.88±0.58, 40.18±1.45, and 2.49±0.02, respectively. These findings indicate that the A2UCOE subregions effectively stabilize transgene expression through epigenetic mechanisms. In contrast, LVs harboring the novel UCOE subregions OFA1, OFA2, and OFA3 (corresponding to 455UCOE, 527UCOE, and 945UCOE vectors) initially supported high levels of transgene expression, but exhibited a substantial decline over time; by day 31, the MFI values had decreased to 1.47±0.54, 3.81±0.62, and 5.91±0.11, respectively. These

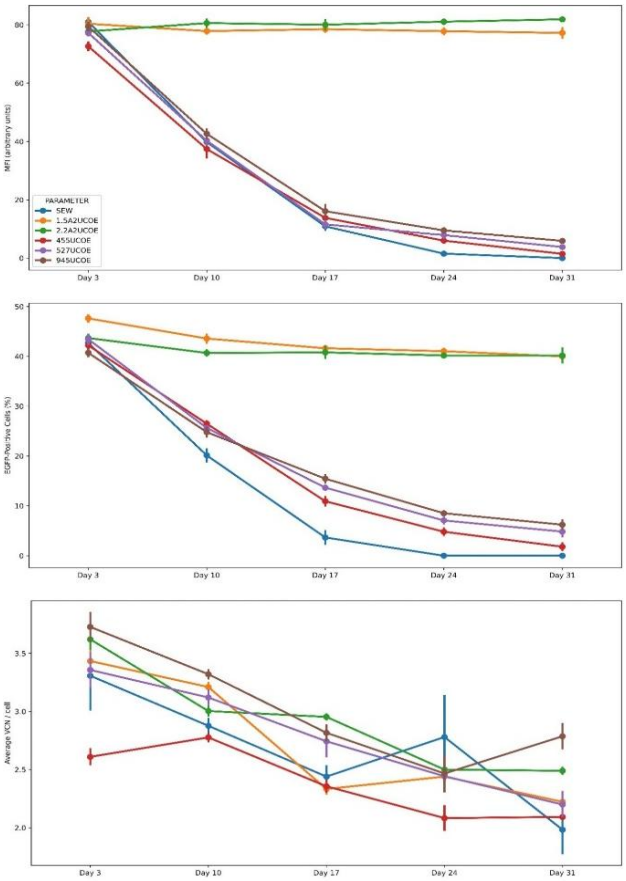


Figure 4. Functional evaluation of the 455UCOE (OFA1), 527UCOE (OFA2), and 945UCOE (OFA3) vectors, comparative analysis of the **A)** MFI, **B)** eGFP+ cells, and **C)** average VCN across different vectors on days 3, 10, 17, 24, and 31 in undifferentiated F9 cells. UCOE: ubiquitous chromatin opening element, MFI: mean fluorescence intensity, eGFP: enhanced green fluorescent protein, VCN: vector copy number

Table 1. Comparison of MFI, eGFP+, and VCN in undifferentiated F9 cells transduced with SEW and UCOE-based LVs

		Day-3	Day-10	Day-17	Day-24	Day-31	p
MFI	**SEW**	80.99±0.74	39.80±0.68	10.90±1.23	1.54±0.36	0.01±0.03^{a}	**0.009**
	1.5A2UCOE	80.37±1.95	77.86±0.93	78.50±0.94	77.82±1.08	77.23±1.61	0.125
	2.2A2UCOE	77.73±1.12	80.60±1.20	80.05±1.61	81.08±0.77^{a}	81.88±0.58^{a}	**0.011**
	455UCOE	72.63±1.32	37.41±2.90^{c}	13.81±1.45^{cf}	6.00±0.54^{cfh}	1.47±0.54^{cfi}	**<0.001**
	527UCOE	72.25±0.94	40.26±1.41^{c}	11.50±1.29^{cf}	7.89±1.06^{cfg}	3.81±0.62^{cfik}	**<0.001**
	945UCOE	79.40±1.36	42.60±1.58^{c}	16.10±2.15^{cf}	9.50±0.82^{cfh}	5.91±0.11^{cfi}	**<0.001**
eGFP	**SEW**	42.67±1.61	20.12±1.24	3.65±1.30	0.00±0.00^{a}	0.00±0.00^{a}	**0.008**
	1.5A2UCOE	47.62±0.65	43.57±0.83^{c}	41.62±0.43^{cd}	41.03±0.48^{ce}	39.99±0.11^{cfg}	**<0.001**
	2.2A2UCOE	43.68±0.42	40.68±0.55^{a}	40.79±1.10^{a}	40.18±0.30^{b}	40.18±1.45^{b}	**0.003**
	455UCOE	42.20±0.33	26.49±0.54^{c}	10.92±0.85^{cf}	4.81±0.69^{cfi}	1.80±0.69^{cfik}	**<0.001**
	527UCOE	43.44±0.96	25.64±0.39^{c}	13.66±0.48^{cf}	7.08±0.59^{cfi}	4.84±0.95^{cfij}	**<0.001**
	945UCOE	40.17±0.71	24.79±0.95	15.44±0.75	8.52±0.36	6.22±0.88^{c}	**0.009**
VCN	**SEW**	3.31±0.29	2.87±0.05	2.44±0.09^{b}	2.78±0.35	1.98±0.20^{cfk}	**<0.001**
	1.5A2UCOE	3.43±0.13	3.21±0.03	2.33±0.04^{cf}	2.44±0.05^{cf}	2.22±0.08^{cf}	**<0.001**
	2.2A2UCOE	3.62±0.08	3.03±0.04	2.95±0.02	2.50±0.08	2.49±0.02^{a}	**0.013**
	455UCOE	2.61±0.06	2.77±0.03	2.35±0.04	2.08±0.10^{d}	2.09±0.01	**0.012**
	527UCOE	3.35±0.14	3.12±0.06	2.74±0.12^{cd}	2.44±0.12^{cf}	2.20±0.10^{cfh}	**<0.001**
	945UCOE	3.72±0.12	3.32±0.03^{b}	2.81±0.06^{ce}	2.46±0.15c^{fh}	2.78±0.10^{cfj}	**<0.001**

MFI: mean fluorescence intensity, eGFP: enhanced green fluorescent protein, VCN: vector copy number, UCOE: ubiquitous chromatin opening element, LV: lentiviral vector, to facilitate comparison, mean and standard deviation values were provided for all parameters, superscript letters denote statistically significant differences according to the post-hoc test results when compared to Day-3 ^{a}: p<0.05, ^{b}: p<0.01, and ^{c}: p<0.001, compared to Day-10 ^{d}: p<0.05, ^{e}: p<0.01, and ^{f}: p<0.001, compared to Day-17 ^{g}: p<0.05, ^{h}: p<0.01, and ^{i}: p<0.001, and compared to Day-24 ^{j}: p<0.05, and ^{k}: p<0.01

results suggest that these newly designed UCOE subregions exhibit limited efficacy in maintaining transgene expression stability, particularly in undifferentiated F9 cells.

Differentiated F9 Cells

Transgene expression in cells transduced with the SEW vector diminished rapidly in differentiated F9 cells, as expected; although a high expression level was observed on day 3, MFI decreased by day 17, and expression was completely silenced by day 31, with no detectable eGFP+ cells remaining (Table 2).

The results demonstrated that in differentiated F9 cells, the positive control vectors (1.5A2UCOE-SEW and 2.2A2UCOE) maintained robust transgene expression, whereas the newly developed constructs (OFA1, OFA2, and OFA3) led to a pronounced decline in eGFP expression, comparable to the SEW vector. This trend was paralleled by fluctuations in MFI values, while VCNs remained relatively stable over time (Figure 5).

In contrast, vectors harboring the 1.5A2UCOE and 2.2A2UCOE elements demonstrated superior performance by largely maintaining transgene expression up to day 31. For instance, in cells transduced with the 2.2A2UCOE construct, the MFI decreased only slightly from 79.90±0.68 on day 3 to 76.48±0.50 on day 31, while the percentage of eGFP+ cells declined from 42.66±0.56 to 38.81±0.33, and the VCN remained stable at 1.93±0.15. In contrast, significant reductions in both MFI and eGFP+ cell percentages were observed over time in the groups transduced with the 455UCOE (OFA1), 527UCOE (OFA2), and 945UCOE (OFA3) constructs ($p<0.001$).

P19 Cell Line Findings

Undifferentiated P19 Cells

In P19 cells, the SEW vector initially induced high levels of eGFP expression (43.34±6.67) and MFI (81.22±2.58) by day 3. However, a dramatic silencing was observed by

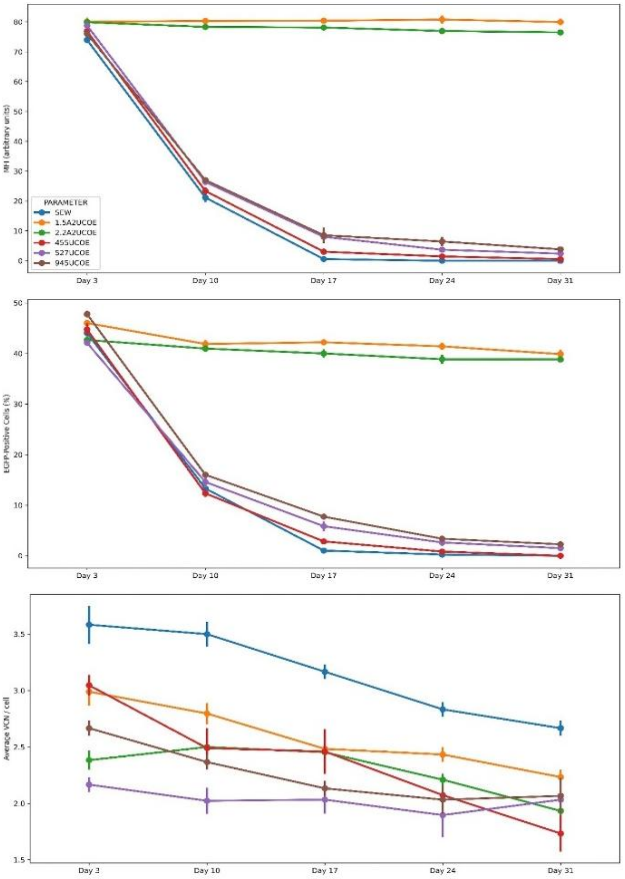


Figure 5. Functional evaluation of the 455UCOE (OFA1), 527UCOE (OFA2), and 945UCOE (OFA3) vectors, comparative analysis of the **A)** MFI, **B)** eGFP+ cells, and **C)** average VCN across different vectors on days 3, 10, 17, 24, and 31 in differentiated F9 cells. UCOE: ubiquitous chromatin opening element, MFI: mean fluorescence intensity, eGFP: enhanced green fluorescent protein, VCN: vector copy number

Table 2. Comparison of MFI, eGFP+, and VCN in differentiated F9 cells transduced with SEW and UCOE-based LVs

		Day-3	Day-10	Day-17	Day-24	Day-31	p
MFI	**SEW**	73.96±0.72	21.16±1.10	0.56±0.20	0.00±0.00[a]	0.00±0.00[a]	**0.008**
	1.5A2UCOE	80.06±1.01	80.31±0.09	80.39±0.29	80.79±0.98	79.90±0.78	0.682
	2.2A2UCOE	79.90±0.68	78.32±0.07	78.11±0.60[a]	76.97±0.74[c]	76.48±0.50[cd]	**<0.001**
	455UCOE	76.89±0.36	23.36±0.95[c]	3.03±0.73[cf]	1.46±0.32[cf]	0.55±0.49[cfh]	**<0.001**
	527UCOE	78.79±0.60	26.40±0.63[c]	8.03±1.20[cf]	3.70±0.10[cfi]	2.39±0.44[cfi]	**<0.001**
	945UCOE	76.05±0.86	27.01±0.31[c]	8.54±2.27[cf]	6.46±1.25[cf]	3.82±0.58[cfg]	**<0.001**
eGFP	**SEW**	44.04±0.42	13.30±0.77	1.03±0.16	0.23±0.15	0.00±0.00[b]	**0.009**
	1.5A2UCOE	46.01±0.50	41.87±0.53[c]	42.20±0.34[c]	41.41±0.51[c]	39.87±0.66[cej]	**<0.001**
	2.2A2UCOE	42.66±0.56	40.96±0.50[a]	39.99±0.63[b]	38.85±0.71[cd]	38.81±0.33[ce]	**<0.001**
	455UCOE	44.74±1.14	12.33±0.51	2.83±0.15	0.83±0.28	0.00±0.00[a]	**0.009**
	527UCOE	42.10±0.43	14.58±0.80	5.84±0.76	2.63±0.46	1.50±0.10[a]	**0.009**
	945UCOE	47.78±0.49	16.01±0.18	7.73±0.13	3.36±0.20	2.26±0.05[a]	**0.009**
VCN	**SEW**	3.58±0.16	3.50±0.10	3.16±0.58	2.83±0.58	2.66±0.58[a]	**0.011**
	1.5A2UCOE	2.99±0.11	2.79±0.09	2.48±0.12	2.43±0.05	2.23±0.05[a]	**0.012**
	2.2A2UCOE	2.38±0.07	2.50±0.10	2.45±0.17	2.21±0.04	1.93±0.15[aeh]	**0.001**
	455UCOE	3.04±0.08	2.49±0.17	2.46±0.19	2.07±0.05	1.73±0.15[a]	**0.012**
	527UCOE	2.17±0.05	2.02±0.10	2.03±0.10	1.89±0.18	2.03±0.05	0.162
	945UCOE	2.67±0.06	2.36±0.06	2.13±0.06	2.03±0.11[a]	2.06±0.15	**0.020**

MFI: mean fluorescence intensity, eGFP: enhanced green fluorescent protein, VCN: vector copy number, UCOE: ubiquitous chromatin opening element, LV: lentiviral vector, to facilitate comparison, mean and standard deviation values were provided for all parameters, superscript letters denote statistically significant differences according to the post-hoc test results when compared to Day-3 [a]: $p<0.05$, [b]: $p<0.01$, and [c]: $p<0.001$, compared to Day-10 [d]: $p<0.05$, [e]: $p<0.01$, and [f]: $p<0.001$, compared to Day-17 [g]: $p<0.05$, [h]: $p<0.01$, and [i]: $p<0.001$, and compared to Day-24 [j]: $p<0.05$

day 31. In contrast, A2UCOE subregions, particularly 2.2A2UCOE, demonstrated marked superiority in maintaining transgene expression. MFI levels decreased only slightly from 80.06±1.62 on day 3 to 76.88±0.49 on day 31, while the percentage of eGFP+ cells declined marginally from 42.67±0.42 to 40.85±0.18, and the VCN remained relatively stable at 1.49±0.02. Similarly, 1.5A2UCOE maintained high expression stability, with a VCN of 1.59±0.04 measured on day 31. In contrast, the OFA1 and OFA3 constructs (455UCOE and 945UCOE, respectively) exhibited diminished performance over time in this cell line (Table 3).

In P19 cells, 1.5A2UCOE-SEW and 2.2A2UCOE constructs maintained stable eGFP expression, MFI levels, and VCNs throughout the observation period, whereas SEW and the novel OFA1, OFA2, and OFA3 constructs showed substantial declines across all parameters. eGFP expression dropped by 80% in SEW-transduced cells and by 60-70% in OFA-transduced cells within two weeks, highlighting the superior stability conferred by A2UCOE elements (Figure 6).

Differentiated P19 Cells

In differentiated P19 cells, transgene expression under the control of the SEW vector was rapidly decreased; the MFI value was 79.30±0.65 on day 3, and silenced on day 31. In contrast, A2UCOE derivatives significantly prevented this loss of expression. Notably, the 2.2A2UCOE vector conferred substantial stability by day 31, maintaining an MFI of 77.81±0.15, an eGFP+ cell ratio of 37.15±0.28, and a VCN of 2.03±0.15. Similarly, the 1.5A2UCOE construct demonstrated a protective effect, with an average VCN remaining at approximately 2.33±0.11. On the other hand, although the 527UCOE and 945UCOE vectors initially achieved high expression levels, a marked decline in these parameters was observed starting from day 17. These findings indicate that A2UCOE derivatives exhibit superior performance in sustaining transgene expression in differentiated P19 cells (Table 4).

P19 cells transduced with the positive control vectors, 1.5A2UCOE-SEW and 2.2A2UCOE, maintained stable eGFP expression and consistent MFI levels following differentiation into the neural ectodermal lineage, whereas cells transduced with the OFA1 (455UCOE), OFA2 (527UCOE), OFA3 (945UCOE), and SEW vectors exhibited a marked decline in both eGFP+ cell frequency and MFI values. Despite these differences in expression levels, average VCN remained relatively constant across all groups (Figure 7).

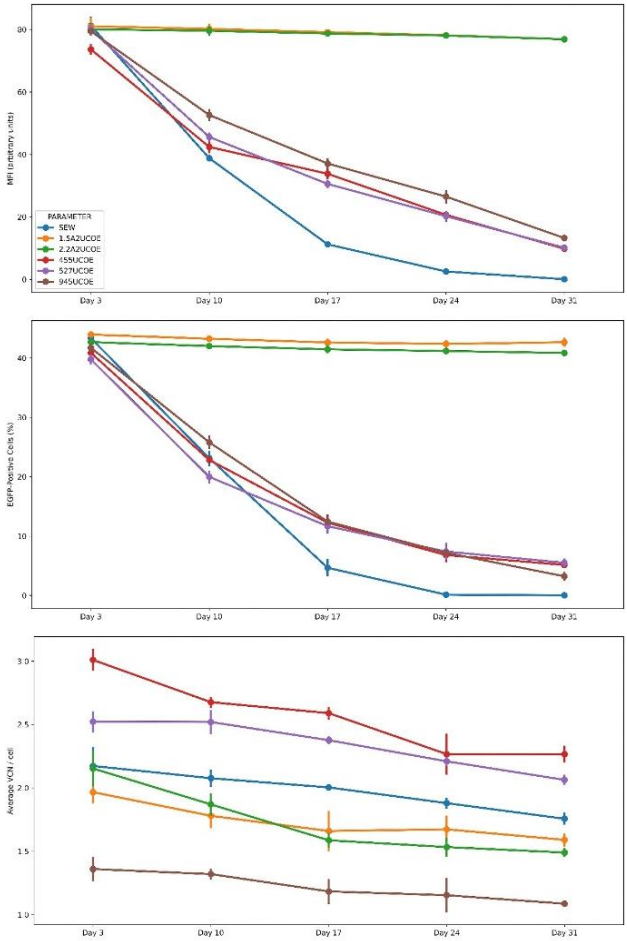


Figure 6. Functional evaluation of the 455UCOE (OFA1), 527UCOE (OFA2), and 945UCOE (OFA3) vectors, comparative analysis of the **A)** MFI, **B)** eGFP+ cells, and **C)** average VCN across different vectors on days 3, 10, 17, 24, and 31 in undifferentiated P19 cells. UCOE: ubiquitous chromatin opening element, MFI: mean fluorescence intensity, eGFP: enhanced green fluorescent protein, VCN: vector copy number

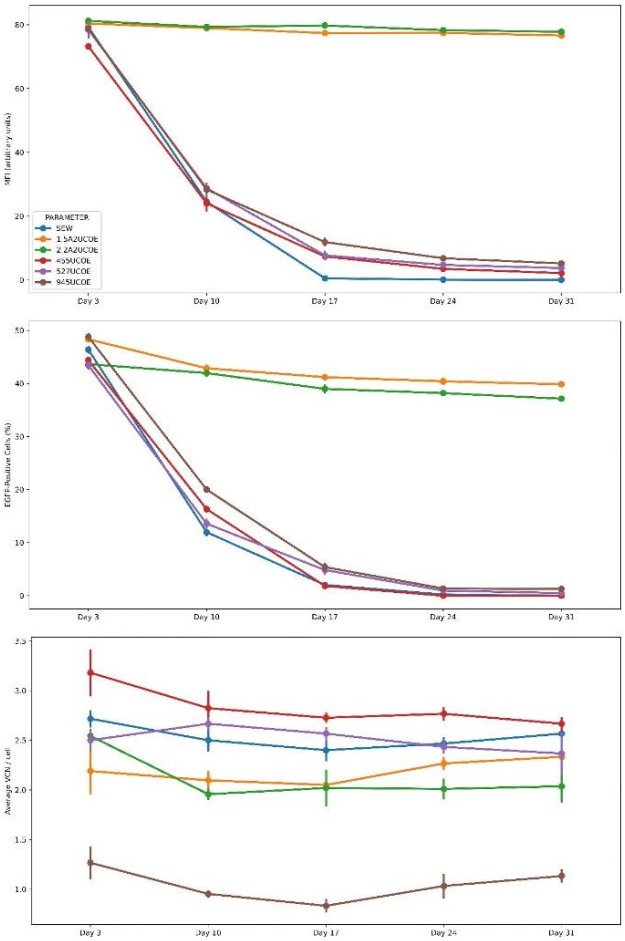


Figure 7. Functional evaluation of the 455UCOE (OFA1), 527UCOE (OFA2), and 945UCOE (OFA3) vectors, comparative analysis of the **A)** MFI, **B)** eGFP+ cells, and **C)** average VCN across different vectors on days 3, 10, 17, 24, and 31 in differentiated P19 cells. UCOE: ubiquitous chromatin opening element, MFI: mean fluorescence intensity, eGFP: enhanced green fluorescent protein, VCN: vector copy number

Table 3. Comparison of MFI, eGFP+, and VCN in undifferentiated P19 cells transduced with SEW and UCOE-based LVs

		Day-3	Day-10	Day-17	Day-24	Day-31	p
MFI	**SEW**	81.22±2.58	38.80±0.60^{c}	11.23±0.60^{cf}	2.54±0.36^{cfi}	0.06±0.02^{cfi}	**<0.001**
	1.5A2UCOE	81.03±2.44	80.19±1.33	79.16±0.58	78.15±0.43	76.90±0.60^{a}	**0.022**
	2.2A2UCOE	80.06±1.62	79.60±1.20	78.71±0.48	78.08±0.35	76.88±0.49^{a}	**0.017**
	455UCOE	73.63±1.32	42.41±1.68^{c}	33.81±1.45^{cf}	20.66±0.80^{cfi}	9.81±0.62^{cfil}	**<0.001**
	527UCOE	79.91±1.50	45.59±1.07^{c}	30.57±0.96^{cf}	20.22±1.47^{cfi}	10.15±0.11^{cfil}	**<0.001**
	945UCOE	79.43±0.63	52.62±1.58^{c}	37.10±1.39^{cf}	26.50±1.80^{cfi}	13.25±0.55^{cfil}	**<0.001**
eGFP	**SEW**	43.34±6.67	23.12±1.13^{c}	4.65±1.29^{cf}	0.13±0.06^{cfi}	0.02±0.01^{cfi}	**<0.001**
	1.5A2UCOE	43.95±0.13	43.24±0.36	42.62±0.43^{a}	42.37±0.43^{a}	42.65±0.59^{a}	**0.007**
	2.2A2UCOE	42.67±0.42	42.01±0.31	41.46±0.51^{a}	41.18±0.30^{b}	40.85±0.18^{b}	**<0.001**
	455UCOE	40.87±0.45	22.82±0.39^{c}	12.26±1.22^{cf}	6.81±1.04^{cfi}	5.13±0.16^{cfi}	**<0.001**
	527UCOE	39.77±0.70	19.97±0.93^{c}	11.66±1.03^{cf}	7.40±1.26^{cfh}	5.50±0.57^{cfi}	**<0.001**
	945UCOE	41.71±0.57	25.79±0.95^{c}	12.44±0.50^{cf}	7.19±0.36^{cfi}	3.22±0.59^{cfi}	**<0.001**
VCN	**SEW**	2.17±0.14	2.07±0.06	2.00±0.00	1.88±0.03	1.75±0.04^{a}	**0.011**
	1.5A2UCOE	1.96±0.08	1.78±0.08	1.66±0.15^{a}	1.67±0.10^{a}	1.59±0.04^{b}	**0.007**
	2.2A2UCOE	2.15±0.13	1.87±0.07^{a}	1.58±0.05^{cd}	1.53±0.06^{ce}	1.49±0.02^{ce}	**<0.001**
	455UCOE	3.01±0.08	2.67±0.03	2.59±0.04	2.67±0.15^{a}	2.67±0.06^{a}	**0.012**
	527UCOE	2.52±0.07	2.52±0.08	2.37±0.02	2.21±0.03^{cfg}	2.06±0.03^{cfi}	**<0.001**
	945UCOE	1.36±0.08	1.32±0.03	1.18±0.09	1.15±0.12	1.08±0.00	0.056

MFI: mean fluorescence intensity, eGFP: enhanced green fluorescent protein, VCN: vector copy number, UCOE: ubiquitous chromatin opening element, LV: lentiviral vector, to facilitate comparison, mean and standard deviation values were provided for all parameters, superscript letters denote statistically significant differences according to the post-hoc test results when compared to Day-3 ^{a}: p<0.05, ^{b}: p<0.01, and ^{c}: p<0.001, compared to Day-10 ^{d}: p<0.05, ^{e}: p<0.01, and ^{f}: p<0.001, compared to Day-17 ^{g}: p<0.05, ^{h}: p<0.01, and ^{i}: p<0.001, and compared to Day-24 ^{l}: p<0.001

Table 4. Comparison of MFI, eGFP+, and VCN in differentiated P19 cells transduced with SEW and UCOE-based LVs

		Day-3	Day-10	Day-17	Day-24	Day-31	p
MFI	**SEW**	79.30±0.65	24.49±0.64	0.48±0.14	0.09±0.01	0.01±0.00^{a}	**0.009**
	1.5A2UCOE	80.39±1.07	78.97±0.63	77.39±0.29^{b}	77.46±0.50^{b}	76.63±0.22^{ce}	**<0.001**
	2.2A2UCOE	81.23±0.73	79.32±0.07^{c}	79.78±0.08^{b}	78.30±0.17^{ch}	77.81±0.15^{cei}	**<0.001**
	455UCOE	73.22±0.67	24.03±2.27^{c}	7.37±0.43^{cf}	3.46±0.33^{cfh}	2.12±0.05^{cfh}	**<0.001**
	527UCOE	78.46±2.48	28.73±0.89^{c}	7.70±1.22^{cf}	4.70±0.10^{cf}	3.72±0.14^{cfg}	**<0.001**
	945UCOE	78.72±0.57	28.35±1.84^{c}	11.88±0.99^{cf}	6.80±0.19^{cfi}	5.16±0.28^{cfi}	**<0.001**
eGFP	**SEW**	46.38±0.51	11.97±0.62	2.03±0.16	0.23±0.15	0.00±0.00^{a}	**0.009**
	1.5A2UCOE	48.34±0.42	42.87±0.53	41.20±0.34	40.41±0.51	39.87±0.34^{a}	**0.010**
	2.2A2UCOE	43.66±0.56	41.97±0.50^{a}	38.99±0.63^{cf}	38.19±0.33^{cf}	37.15±0.28^{cfh}	**<0.001**
	455UCOE	44.41±0.48	16.33±0.50	1.87±0.15	0.00±0.00^{a}	0.00±0.00^{a}	**0.008**
	527UCOE	43.43±0.57	13.58±0.80	4.84±0.76	0.96±0.11	0.50±0.10^{a}	**0.009**
	945UCOE	48.78±0.50	20.01±0.19	5.40±0.62	1.36±0.20	1.26±0.06^{a}	**0.011**
VCN	**SEW**	2.71±0.07	2.50±0.10	2.40±0.10^{a}	2.46±0.06	2.56±0.06	**0.039**
	1.5A2UCOE	2.12±0.22	2.09±0.08	2.05±0.13	2.26±0.05	2.33±0.11	0.127
	2.2A2UCOE	2.54±0.06	1.95±0.04^{b}	2.02±0.17^{b}	2.01±0.09^{b}	2.03±0.15^{b}	**<0.001**
	455UCOE	3.18±0.22	2.82±0.16	2.72±0.04	2.76±0.05	2.66±0.05	0.063
	527UCOE	2.50±0.10	2.66±0.05	2.56±0.05	2.43±0.05	2.36±0.20	0.085
	945UCOE	1.26±0.15	0.95±0.02	0.83±0.05^{a}	1.03±0.11	1.13±0.05	**0.024**

MFI: mean fluorescence intensity, eGFP: enhanced green fluorescent protein, VCN: vector copy number, UCOE: ubiquitous chromatin opening element, LV: lentiviral vector, to facilitate comparison, mean and standard deviation values were provided for all parameters, superscript letters denote statistically significant differences according to the post-hoc test results when compared to Day-3 ^{a}: p<0.05, ^{b}: p<0.01, and ^{c}: p<0.001, compared to Day-10 ^{e}: p<0.01, and ^{f}: p<0.001, compared to Day-17 ^{g}: p<0.05, ^{h}: p<0.01, and ^{i}: p<0.001

Vector Copy Number (VCN) Analysis

qPCR analysis of VCN from genomic DNA demonstrated that the A2UCOE subregions maintained vector genomic integration and copy number stability significantly over time. Analyses conducted in both differentiated and undifferentiated states of F9 and P19 cell lines revealed significant reductions in VCN after differentiation in SEW and OFA1, OFA2, and OFA3 vectors. In contrast, vectors containing 1.5A2UCOE and 2.2A2UCOE preserved VCN stability at high levels regardless of differentiation status in both cell lines, providing significant protection (p=0.012 for 1.5A2UCOE and p=0.001 for 2.2A2UCOE in differentiated F9 cells; and p=0.007 and p<0.001, respectively, in undifferentiated P19 cells).

Moreover, in undifferentiated F9 cells, average VCN values remained stable at 3.43±0.13 and 3.62±0.08 in the 1.5A2UCOE and 2.2A2UCOE groups, respectively, while significant decreases were observed in the SEW group ($p<0.001$). Similarly, in differentiated cells, VCN values in the 1.5A2UCOE and 2.2A2UCOE groups remained significantly higher compared to other vectors, preserving transgene stability. Throughout the experimental period, no significant changes were detected in the average VCN per cell, indicating that no substantial loss of vector occurred relative to the MOI used during transfection.

These findings demonstrate that the A2UCOE subregions support long-term maintenance of vector genomes and sustained transgene expression through epigenetic regulatory mechanisms. Statistically supported, these results indicate that vectors containing the 1.5A2UCOE and 2.2A2UCOE constructs significantly mitigate differentiation-associated epigenetic silencing effects, thereby enhancing the persistence of transgene expression.

DISCUSSION

Vector systems that enable stable genomic integration are essential for sustained therapeutic gene incorporation and expression, especially in mitotic stem cells. Over the past fifteen years, clinical applications utilizing these vector systems in ex vivo HSC gene therapies have yielded promising results in treating genetic disorders such as severe combined immunodeficiency (SCID), including SCID-X1 and SCID-ADA (26,27), Wiskott-Aldrich syndrome, and chronic granulomatous disease (28,29). More recently, LVs have shown considerable potential in addressing the inherited demyelinating diseases such as X-linked adrenoleukodystrophy (30), metachromatic leukodystrophy (31), and Wiskott-Aldrich syndrome (32). Despite these advances, two major challenges remain critical concerns in the use of these integrative viral vectors: insertional mutagenesis and epigenetic silencing of the therapeutic transgene (14).

Epigenetic silencing of the gene of interest significantly contributes to decreased productivity over time (33,34). This non-mutational gene inactivation occurs via repressive covalent modifications, such as DNA cytosine methylation and histone posttranslational modifications, which independently or synergistically influence gene transcription (35). Many studies have highlighted aberrant DNA methylation and hypoacetylation of histone H3 as contributing to variegated transgene expression or complete silencing over time (36,38). While previous research has demonstrated that UCOEs can maintain open chromatin conformation and stable transgene expression via bidirectional promoter activity (18), emerging evidence indicates that promoterless CpG-rich sequences may also facilitate chromatin opening and DNA demethylation, thereby counteracting epigenetic silencing (23). This study aimed to evaluate whether the CpG-rich, promoterless subregions OFA1, OFA2, and OFA3 from the A2UCOE locus can sustain UCOE-like functions and maintain stable transgene expression. Contrary to initial hypotheses, these fragments failed to maintain stable expression in both undifferentiated and differentiated murine embryonal carcinoma cell lines (P19 and F9). Results showed a faster decline of transgene expression in differentiated cells compared to undifferentiated cells. This could be attributed to the more complex and dynamic epigenetic remodeling that occurs during differentiation, which often leads to enhanced DNA methylation and histone modifications that silence transgene promoters more efficiently. Differentiated cells may thus present a more repressive chromatin environment, accelerating transgene silencing compared to pluripotent or less differentiated states. The rates of transgene silencing were comparable to the control vector containing only the SFFV promoter, indicating the absence of a UCOE within these promoterless CpG-rich regions.

Some studies have questioned whether promoter activity is necessary for UCOE function. Bandaranayake et al. (39) demonstrated that a 700 bp promoterless CBX3 fragment could stabilize expression in CHO cells, but only at high VCNs. The results suggest that this apparent stability is likely due to high copy number, as silencing occurred over time at typical low vector doses. Testing the highly CpG-dense subregions of A2UCOE (455UCOE, 527UCOE, and 945UCOE) upstream of an SFFV promoter, none were found to confer expression stability in P19 and F9 cells. This indicates that CpG density alone is insufficient to maintain an open chromatin structure, and promoter-associated transcriptional activity or sufficient fragment length may be required for full UCOE function (18).

The primary aim of the present study was to assess whether sub-regions of the human HNRPA2B1 CBX3-derived A2UCOE retain UCOE function. Previous studies showed that CpG island fragments, some lacking promoters, maintain DNA methylation in a transgene context (40), questioning the dual divergent transcription model of UCOE (18). The 455UCOE, 527UCOE, and 945UCOE LVs contain promoter-free, CpG-rich fragments downstream of CBX3's two alternative first exons. It was hypothesized that these fragments could establish open chromatin independently and stabilize expression from a linked SFFV promoter (23). However, in both undifferentiated and differentiated P19 and F9 cells, none conferred expression stability compared to the positive A2UCOE control, indicating a lack of UCOE function.

To clarify whether the decline in transgene expression resulted from loss of vector-positive cells or transcriptional silencing, qPCR was performed at multiple time points post-transduction to measure average VCN per cell. A reference cell clone harboring a single vector copy was used for normalization. The results demonstrated that VCN remained stable throughout the culture period, indicating that vector loss did not occur. However, the percentage of GFP+ cells declined only in vectors containing the tested UCOE sub-fragments, while remaining constant in control groups. This suggests that the reduction in expression was attributable to transcriptional silencing rather than a decrease in VCN (41). These findings support that the promoterless but CpG-rich subregions, 455UCOE, 527UCOE, and 945UCOE, derived from the human HNRPA2B1-CBX3 locus do not exhibit UCOE activity. Although previous studies proposed that promoterless CpG islands could establish open chromatin and prevent DNA methylation (42), the results showed that these fragments failed to maintain stable expression. This indicates that high CpG density alone is insufficient and that promoter-associated transcriptional activity may be essential for UCOE function (43).

Insertional mutagenesis occurs when the integration of gammaretroviral vectors inadvertently activates host cell proto-oncogenes, a complication reported in five out of twenty patients treated for SCID-X1 (26,27). Conversely, transgene silencing, attributed to DNA methylation of the promoter region, led to the eventual failure of initially effective gene therapy in two chronic granulomatous disease patients. In this study, the subregions OFA1, OFA2, and OFA3, derived from the human HNRPA2B1-CBX3 locus and characterized by promoterless but CpG-rich sequences, were investigated to assess their ability to maintain UCOE functionality. Experimental data demonstrated that these subregions failed to sustain stable transgene expression in both undifferentiated and differentiated P19 and F9 cell lines; the rates of transgene silencing were comparable to those observed with the control vector containing only the SFFV promoter. These results suggest that these promoterless CpG-rich regions lack UCOE activity. However, a critical limitation of this study is the absence of direct epigenetic profiling, such as analyses of DNA methylation and histone modifications, which hinders full elucidation of the mechanisms underlying the observed lack of UCOE activity. Previous studies have shown that CpG density alone does not guarantee chromatin accessibility or transcriptional activity; rather, the interplay between DNA methylation, histone acetylation, and chromatin remodeler recruitment is essential. For instance, promoterless CpG islands may remain methylated or fail to recruit activating histone marks, thereby losing their capacity to maintain an open chromatin state despite high CpG content (44,45). Moreover, RNA polymerase II-mediated bidirectional transcription has been proposed to prevent DNA methylation and promote an accessible chromatin environment (18). Future investigations incorporating bisulfite sequencing, chromatin immunoprecipitation (ChIP) for histone marks such as H3K4me3 and H3K27ac, and an assay for transposase-accessible chromatin using sequencing (ATAC-seq) will provide valuable insights into the epigenetic landscape of these UCOE subregions. Such analyses could clarify whether the absence of promoter activity alone accounts for their failure to sustain stable transgene expression or if additional epigenetic modifications contribute.

CONCLUSION

This study aimed to investigate whether the CpG-rich, promoterless subregions OFA1, OFA2, and OFA3 from the human A2UCOE locus can maintain stable transgene expression by resisting epigenetic silencing. While CpG-rich sequences remain a promising feature for chromatin opening elements, the findings emphasize that CpG density without promoter-associated transcriptional activity is insufficient to confer stable UCOE function. This underscores the complexity of epigenetic regulation and the necessity of integrating comprehensive epigenomic analyses to better understand and harness UCOE mechanisms for gene therapy applications.

Although the tested CpG-rich, promoterless subregions did not exhibit UCOE activity, representing negative experimental outcomes, this study provides valuable insight by confirming that CpG density alone is insufficient to act as a chromatin-opening element and sustain stable transgene expression. Negative results are important as they delineate the functional boundaries of UCOE elements and inform improvements in gene therapy vector design. Furthermore, comparative analyses with the positive control A2UCOE emphasize that promoter-associated activity is more critical than CpG richness in maintaining transgene expression stability.

Future studies should use epigenetic profiling methods like bisulfite sequencing, ChIP for histone marks, and ATAC-seq to clarify UCOE mechanisms. Additionally, investigating how promoter-linked transcription influences chromatin remodeling may help design more effective vectors with stable transgene expression and reduced silencing.

Ethics Committee Approval: Since our study was not an experimental study including human or animal subject, ethics committee approval was not required.

Conflict of Interest: None declared by the authors.

Financial Disclosure: None declared by the authors.

Acknowledgments: We gratefully acknowledge the contributions of Prof. Adrian Thrasher and his colleagues from University College London, UK, to this study. We also gratefully acknowledge the contributions of Prof. Michael Antoniou from King's College London.

Author Contributions: Idea/Concept: AOA, ÖFA; Design: ÖFA; Data Collection/Processing: AOA, ÖFA; Analysis/Interpretation: AOA, ÖFA; Literature Review: AOA, ÖFA; Drafting/Writing: AOA, ÖFA; Critical Review: AOA, ÖFA.

REFERENCES

1. Neville JJ, Orlando J, Mann K, McCloskey B, Antoniou MN. Ubiquitous chromatin-opening elements (UCOEs): Applications in biomanufacturing and gene therapy. Biotechnol Adv. 2017;35(5):557-64.
2. Griesenbach U, Alton EW. Moving forward: cystic fibrosis gene therapy. Hum Mol Genet. 2013;22(R1):R52-8.
3. Bainbridge JW, Tan MH, Ali RR. Gene therapy progress and prospects: the eye. Gene Ther. 2006;13(16):1191-7.
4. Alexander SL, Linde-Zwirble WT, Werther W, Depperschmidt EE, Wilson LJ, Palanki R, et al. Annual rates of arterial thromboembolic events in Medicare neovascular age-related macular degeneration patients. Ophthalmology. 2007;114(12):2174-8.

5. Vogt VM, Simon MN. Mass determination of Rous sarcoma virus virions by scanning transmission electron microscopy. J Virol. 1999;73(8):7050-5.
6. Bouard D, Alazard-Dany N, Cosset FL. Viral vectors: from virology to transgene expression. Br J Pharmacol. 2009;157(2):153-65.
7. Gascón S, Paez-Gomez JA, Díaz-Guerra M, Scheiffele P, Scholl FG. Dual-promoter lentiviral vectors for constitutive and regulated gene expression in neurons. J Neurosci Methods. 2008;168(1):104-12.
8. Yee TT, Pasi KJ, Lilley PA, Lee CA. Factor VIII inhibitors in haemophiliacs: a single-centre experience over 34 years, 1964-97. Br J Haematol. 1999;104(4):909-14.
9. Zaiss AK, Son S, Chang LJ. RNA 3′ readthrough of oncoretrovirus and lentivirus: implications for vector safety and efficacy. J Virol. 2002;76(14):7209-19.
10. Ellis J. Silencing and variegation of gammaretrovirus and lentivirus vectors. Hum Gene Ther. 2005;16(11):1241-6.
11. Yao S, Sukonnik T, Kean T, Bharadwaj RR, Pasceri P, Ellis J. Retrovirus silencing, variegation, extinction, and memory are controlled by a dynamic interplay of multiple epigenetic modifications. Mol Ther. 2004;10(1):27-36.
12. Laker C, Meyer J, Schopen A, Friel J, Heberlein C, Ostertag W, et al. Host cis-mediated extinction of a retrovirus permissive for expression in embryonal stem cells during differentiation. J Virol. 1998;72(1):339-48.
13. Zufferey R, Dull T, Mandel RJ, Bukovsky A, Quiroz D, Naldini L, et al. Self-inactivating lentivirus vector for safe and efficient in vivo gene delivery. J Virol. 1998;72(12):9873-80.
14. Antoniou MN, Skipper KA, Anakok O. Optimizing retroviral gene expression for effective therapies. Hum Gene Ther. 2013;24(4):363-74.
15. Fuks F. DNA methylation and histone modifications: teaming up to silence genes. Curr Opin Genet Dev. 2005;15(5):490-5.
16. Antoniou M, Harland L, Mustoe T, Williams S, Holdstock J, Yague E, et al. Transgenes encompassing dual-promoter CpG islands from the human TBP and HNRPA2B1 loci are resistant to heterochromatin-mediated silencing. Genomics. 2003;82(3):269-79.
17. Williams S, Mustoe T, Mulcahy T, Griffiths M, Simpson D, Antoniou M, et al. CpG-island fragments from the HNRPA2B1/CBX3 genomic locus reduce silencing and enhance transgene expression from the hCMV promoter/enhancer in mammalian cells. BMC Biotechnol. 2005;5:17.
18. Lindahl Allen M, Antoniou M. Correlation of DNA methylation with histone modifications across the HNRPA2B1-CBX3 ubiquitously-acting chromatin open element (UCOE). Epigenetics. 2007;2(4):227-36.
19. Smith J, Sen S, Weeks RJ, Eccles MR, Chatterjee A. Promoter DNA hypermethylation and paradoxical gene activation. Trends Cancer. 2020;6(5):392-406.
20. Bhan A, Deb P, Mandal SS. Epigenetic code: Histone modification, gene regulation, and chromatin dynamics. In: Mandal SS, editor. Gene regulation, epigenetics and hormone signaling. Weinheim, Germany: Wiley-VCH Verlag GmbH & Co. KGaA; 2017. p.29-58.
21. Scharf AN, Barth TK, Imhof A. Establishment of histone modifications after chromatin assembly. Nucleic Acids Res. 2009;37(15):5032-40.
22. Zhou VW, Goren A, Bernstein BE. Charting histone modifications and the functional organization of mammalian genomes. Nat Rev Genet. 2011;12(1):7-18.
23. Thomson JP, Skene PJ, Selfridge J, Clouaire T, Guy J, Webb S, et al. CpG islands influence chromatin structure via the CpG-binding protein Cfp1. Nature. 2010;464(7291):1082-6.
24. Zhang F, Frost AR, Blundell MP, Bales O, Antoniou MN, Thrasher AJ. A ubiquitous chromatin opening element (UCOE) confers resistance to DNA methylation-mediated silencing of lentiviral vectors. Mol Ther. 2010;18(9):1640-9.
25. Zhang F, Thornhill SI, Howe SJ, Ulaganathan M, Schambach A, Sinclair J, et al. Lentiviral vectors containing an enhancer-less ubiquitously acting chromatin opening element (UCOE) provide highly reproducible and stable transgene expression in hematopoietic cells. Blood. 2007;110(5):1448-57.
26. Cavazzana-Calvo M, Fischer A, Hacein-Bey-Abina S, Aiuti A. Gene therapy for primary immunodeficiencies: Part 1. Curr Opin Immunol. 2012;24(5):580-4.
27. Cavazza A, Moiani A, Mavilio F. Mechanisms of retroviral integration and mutagenesis. Hum Gene Ther. 2013;24(2):119-31.
28. Ott MG, Seger R, Stein S, Siler U, Hoelzer D, Grez M. Advances in the treatment of chronic granulomatous disease by gene therapy. Curr Gene Ther. 2007;7(3):155-61.
29. Aiuti A, Bacchetta R, Seger R, Villa A, Cavazzana-Calvo M. Gene therapy for primary immunodeficiencies: Part 2. Curr Opin Immunol. 2012;24(5):585-91.
30. Cartier N, Hacein-Bey-Abina S, Bartholomae CC, Veres G, Schmidt M, Kutschera I, et al. Hematopoietic stem cell gene therapy with a lentiviral vector in X-linked adrenoleukodystrophy. Science. 2009;326(5954):818-23.
31. Biffi A, Montini E, Lorioli L, Cesani M, Fumagalli F, Plati T, et al. Lentiviral hematopoietic stem cell gene therapy benefits metachromatic leukodystrophy. Science. 2013;341(6148):1233158.
32. Bosticardo M, Ferrua F, Cavazzana M, Aiuti A. Gene therapy for Wiskott-Aldrich Syndrome. Curr Gene Ther. 2014;14(6):413-21.
33. Marx N, Eisenhut P, Weinguny M, Klanert G, Borth N. How to train your cell - Towards controlling phenotypes by harnessing the epigenome of Chinese hamster ovary production cell lines. Biotechnol Adv. 2022;56:107924.
34. Bachhav B, de Rossi J, Llanos CD, Segatori L. Cell factory engineering: Challenges and opportunities for synthetic biology applications. Biotechnol Bioeng. 2023;120(9):2441-59.
35. Cabrera A, Edelstein HI, Glykofrydis F, Love KS, Palacios S, Tycko J, et al. The sound of silence: Transgene silencing in mammalian cell engineering. Cell Syst. 2022;13(12):950-73.
36. Sizer RE, White RJ. Use of ubiquitous chromatin opening elements (UCOE) as tools to maintain transgene expression in biotechnology. Comput Struct Biotechnol J. 2022;21:275-83.

37. Fu Y, Han Z, Cheng W, Niu S, Wang T, Wang X. Improvement strategies for transient gene expression in mammalian cells. Appl Microbiol Biotechnol. 2024;108(1):480.
38. Jones PA. Functions of DNA methylation: islands, start sites, gene bodies and beyond. Nat Rev Genet. 2012;13(7):484-92.
39. Zhang F, Thornhill SI, Howe SJ, Ulaganathan M, Schambach A, Sinclair J, et al. Lentiviral vectors containing an enhancer-less ubiquitously acting chromatin opening element (UCOE) provide highly reproducible and stable transgene expression in hematopoietic cells. Blood. 2007;110(5):1448-57.
40. Lienert F, Wirbelauer C, Som I, Dean A, Mohn F, Schübeler D. Identification of genetic elements that autonomously determine DNA methylation states. Nat Genet. 2011;43(11):1091-7.
41. Ma J, Meyer S, Olweus J, Jin C, Yu D. An adjusted droplet digital PCR assay for quantification of vector copy number in CAR-T cell and TCR-T cell products. Immunooncol Technol. 2024;25:101031.
42. Cain JA, Montibus B, Oakey RJ. Intragenic CpG islands and their impact on gene regulation. Front Cell Dev Biol. 2022;10:832348.
43. Sizer RE, White RJ. Use of ubiquitous chromatin opening elements (UCOE) as tools to maintain transgene expression in biotechnology. Comput Struct Biotechnol J. 2022;21:275-83.
44. Cedar H, Bergman Y. Linking DNA methylation and histone modification: patterns and paradigms. Nat Rev Genet. 2009;10(5):295-304.
45. Bird A. DNA methylation patterns and epigenetic memory. Genes Dev. 2002;16(1):6-21.